Squeezing more out of 2D seismic data: Processing and interpretation of a pseudo-3D seismic survey from New Zealand

J. Helen Isaac and Don C. Lawton

helen.isaac@ucalgary.ca

ABSTRACT

During the acquisition of seismic data near Christchurch, New Zealand, in 2011, some receivers along a 2D line were left live to record data from sources located on an orthogonal 2D line. We created a pseudo-3D seismic survey from these data. We processed the data unconventionally to remove shot-generated noise and stacked it into bins having the same dimension as the receiver spacing in order to increase the fold. We interpreted faults on the pseudo-3D data and were able to update the regional fault trend interpreted previously using 2D data integrated with regional mapping.
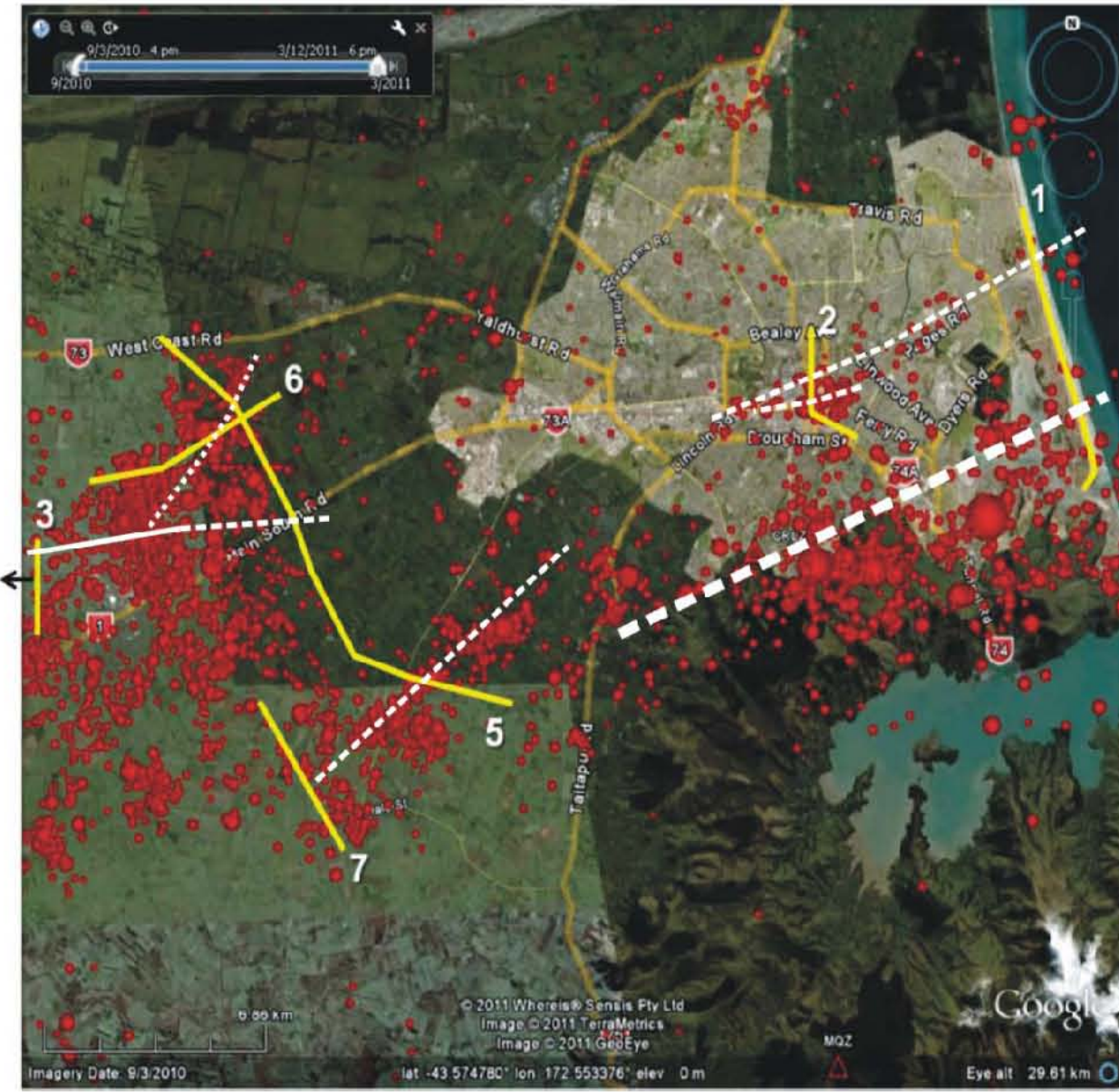
FIG.1: Layout of the 2D seismic lines acquired near Christchurch with interpreted faults in white. The red dots show the epicentres of aftershocks as of June 2011

DATA PROCESSING

221 vibrator points from line 6, spaced 20 m apart, were shot into 120 receivers 10 m apart along orthogonal line 5 (Figure 1). Noise observed in the data has velocity moveout ranging between 170 m/s and 550 m/s. The six representative shots displayed in Figure 2 show how the noise gets shallower in arrival time as the shots get closer to the receiver line and that there are several sources of noise.

We applied several noise attenuation procedures to the data to remove these undesired events. Figures 3 to 6 show the improvement in the signal/noise ratio in the gathers as the processing progresses. All the data include the refraction statics supplied by Sensor from their processing of the 2D lines. The processes we applied include air blast attenuation and predictive deconvolution (Figure 3), further air blast attenuation on receiver gathers and a bandpass filter of 15-20-90-100 Hz (Figure 4), trace equalisation and Gabor deconvolution (Figure 5), and NMO correction, 5-trace mixing of NMO-corrected gathers, NMO removal and a bandpass filter of 5-10-90-100 Hz (Figure 6). Usually one would not expect to apply both predictive deconvolution and Gabor deconvolution or to mix NMO-corrected shot gathers but this non-standard processing stream resulted in the greatest amount of noise attenuation and enhancement of the stacked data.

We 3D binned the data using a bin size of 10x10 m. This size was preferred over a standard 5x5 m bin size (half receiver spacing) as it increased the low CMP fold somewhat. Some CMP bins were empty so after application of NMO and stack we padded the dataset with blank traces then did a 3-trace mix to interpolate the blank traces with data from the two adjacent traces. After this procedure we post-stack migrated the data using a finite-difference algorithm, muted migration smiles and killed padded traces at the ends of the lines. The area covered at a reflection time of 1 s is about 580x1420 m.
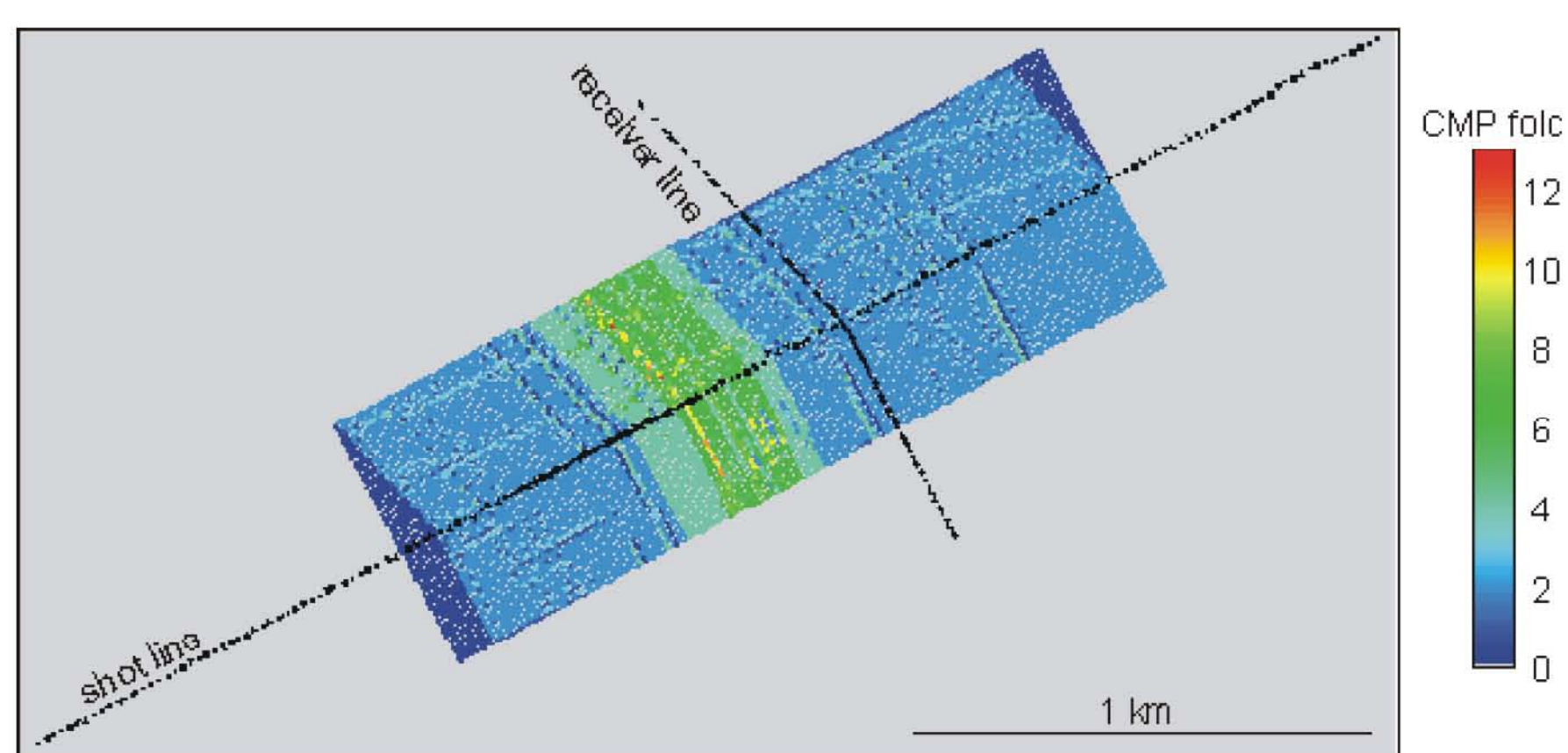

FIG. 7: Plot of CMP bin fold with shot and receiver lines.
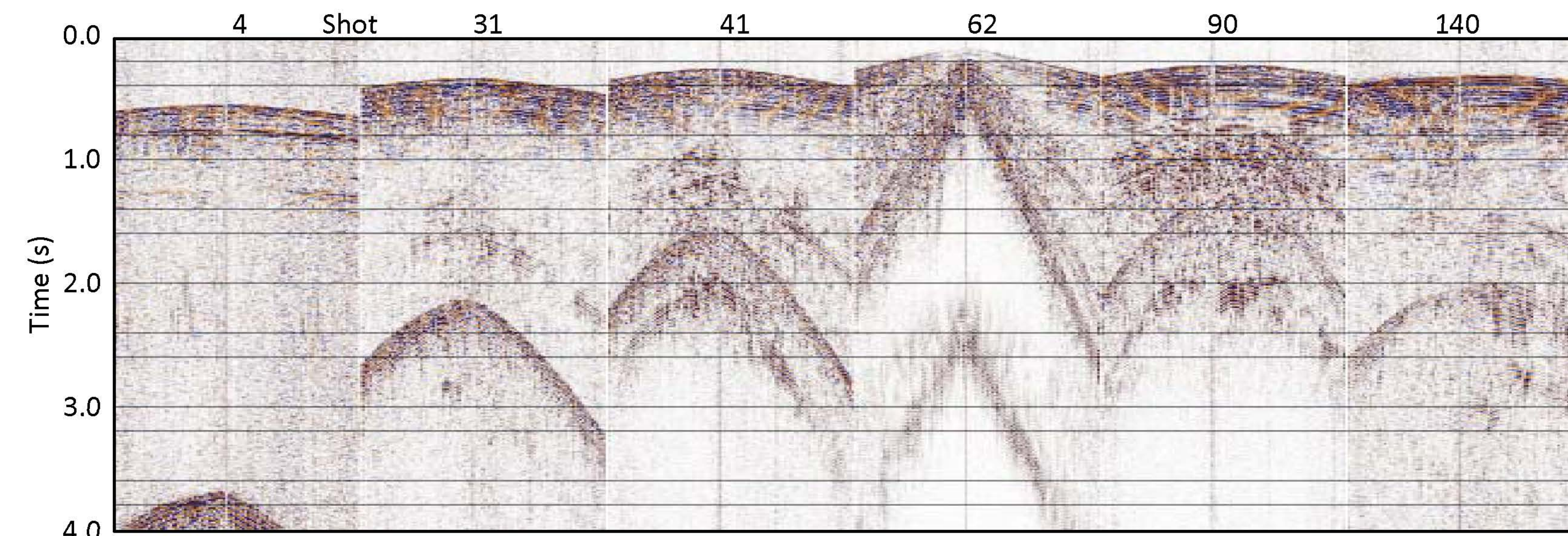

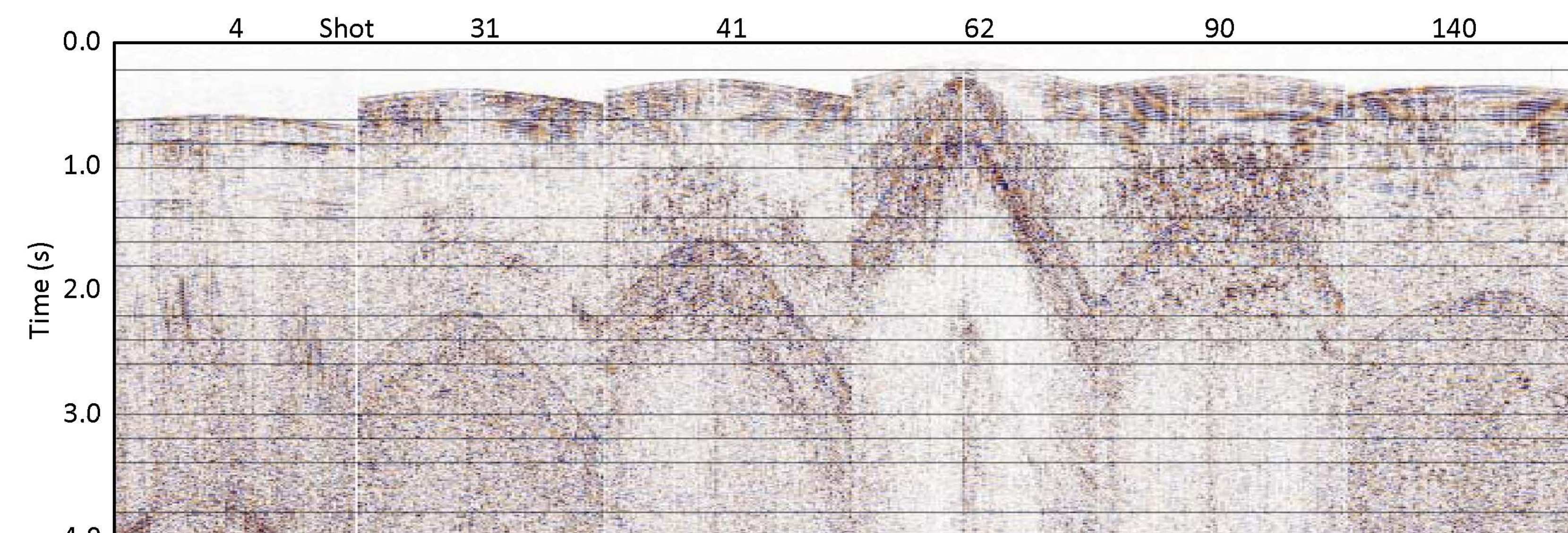FIG. 2: Six representative shots showing different noise patterns.

FIG. 3: The six shots after air blast attenuation and predictive deconvolution.
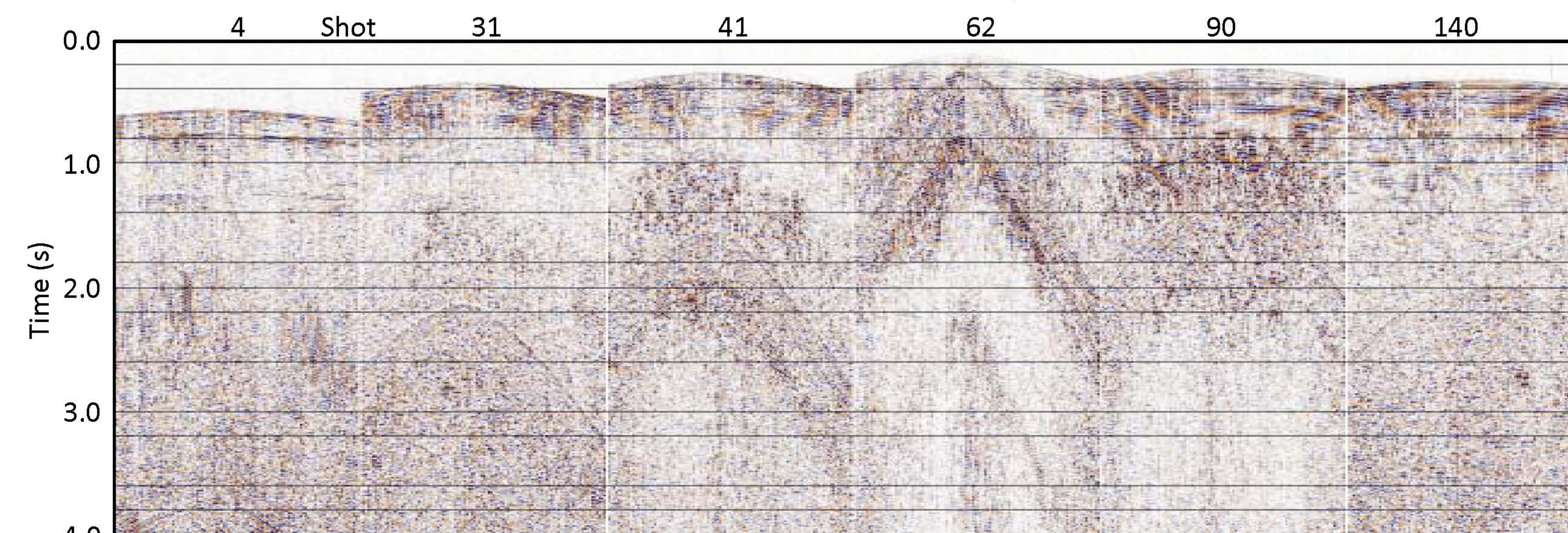

FIG. 4: The six shots after additional air blast attenuation on receiver gathers and bandpass filter of 15-20-90-100 Hz.
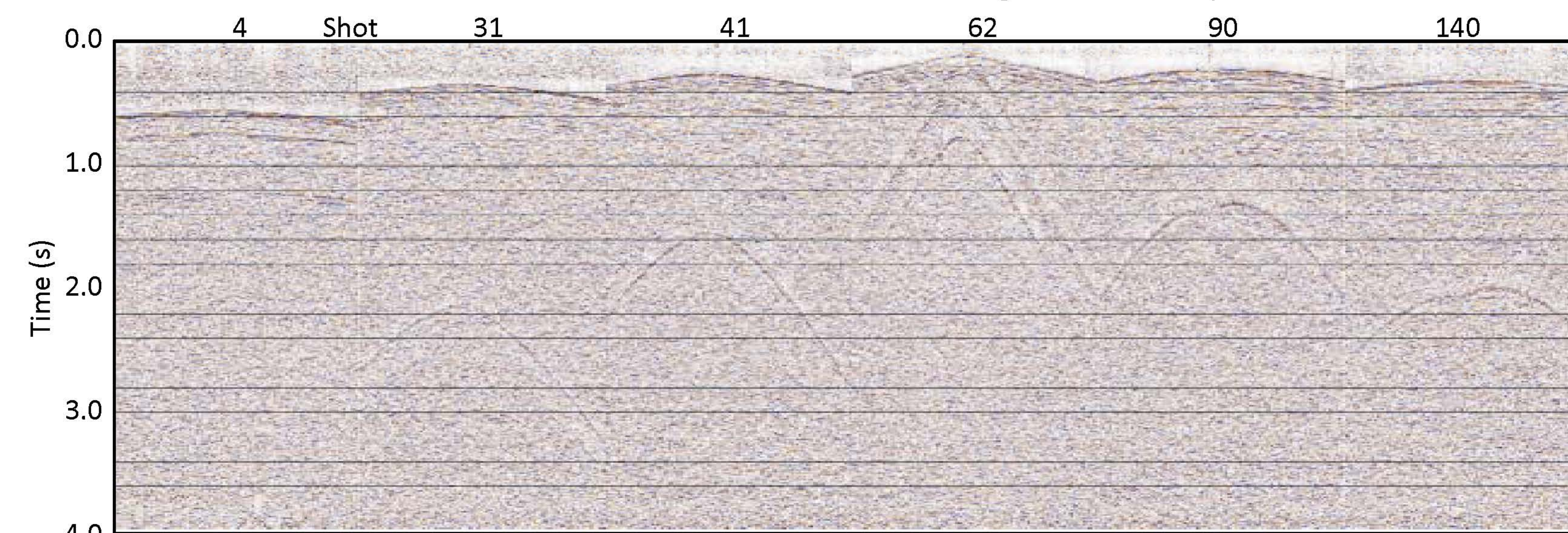

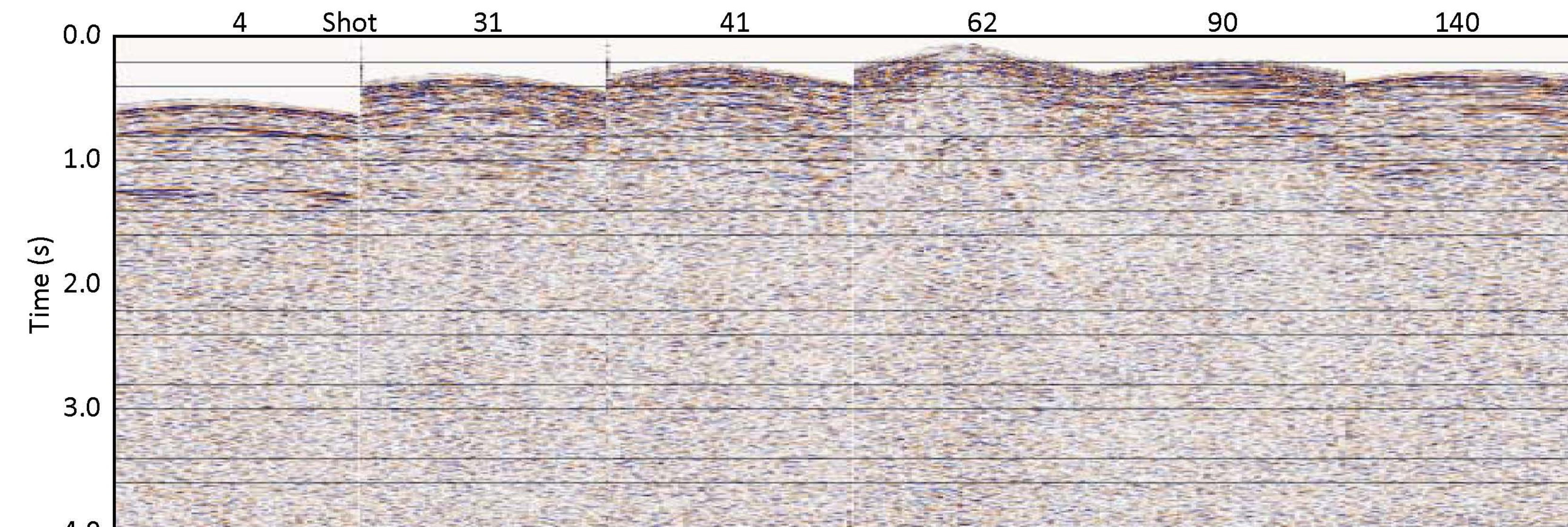FIG. 5: The six shots after Gabor deconvolution.

FIG. 6: The six shots after 5-trace mixing of NMO-corrected gathers, NMO removal and 5-10-90-100 Hz bandpass filter.

The migrated pseudo-3D and the 2D data processed by Sensor were imported into a Kingdom Suite project for interpretation. In Figure 8 we see three semi-parallel lines: crossline 77, Robinson's Road 2D line from cdps 2700 to 2300, and crossline 146. The faults on Robinson's Road line were interpreted by Lawton et al. (2011) and the red fault on the crosslines is interpreted to be the same one as the red fault on Robinson's Road line. The map in Figure 8 shows the displayed lines and the trace of the red fault. Crossline 77 has fold of 6-9 thus is far more reliable than crossline 1467, which has fold of only 1-3. The trend of the red fault is in agreement with the interpreted fault crossing lines 5 and 6 that was shown on Figure 1. We have changed the direction of this fault slightly to reflect the fault trace interpreted on the pseudo-3D data (Figure 9).
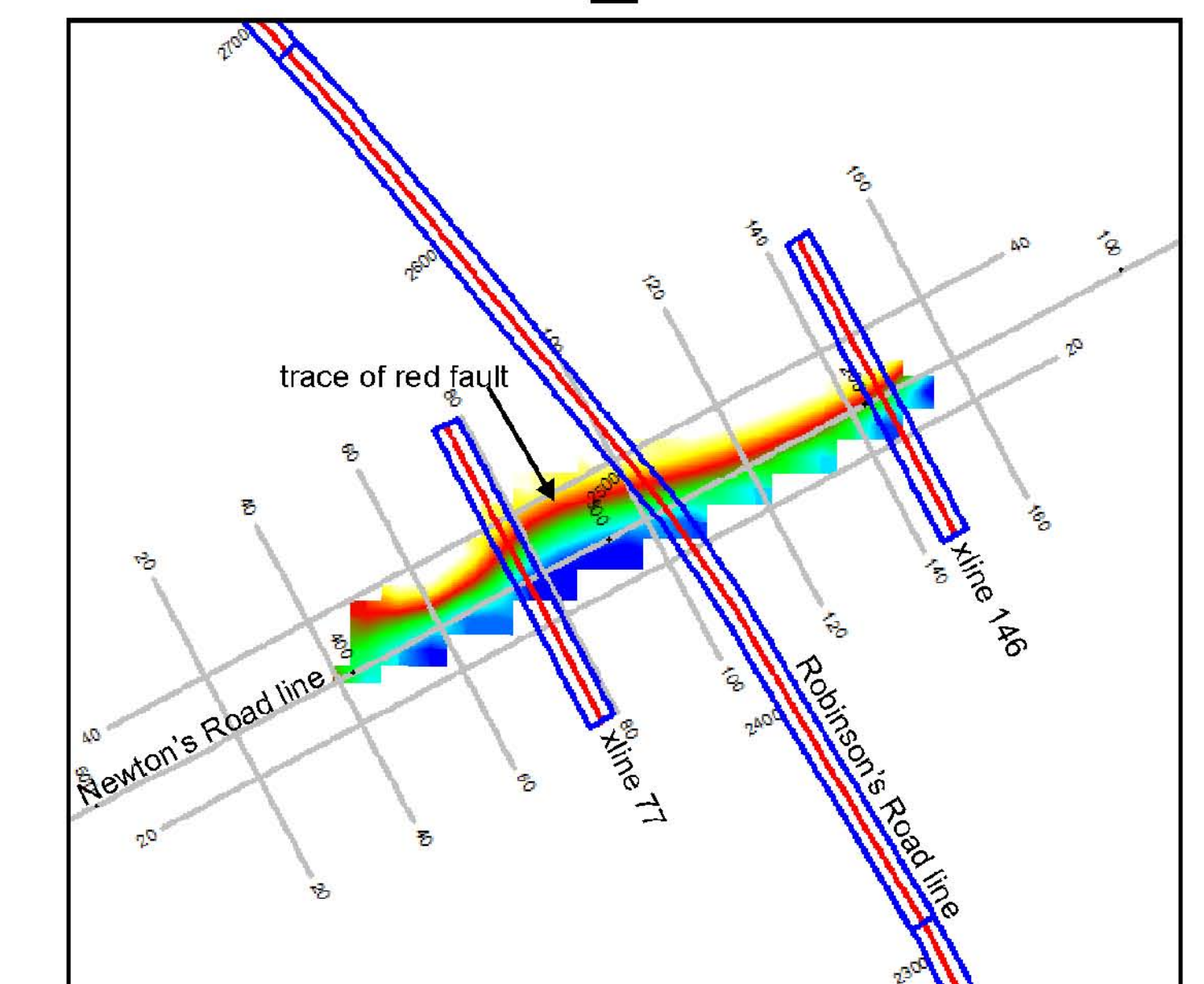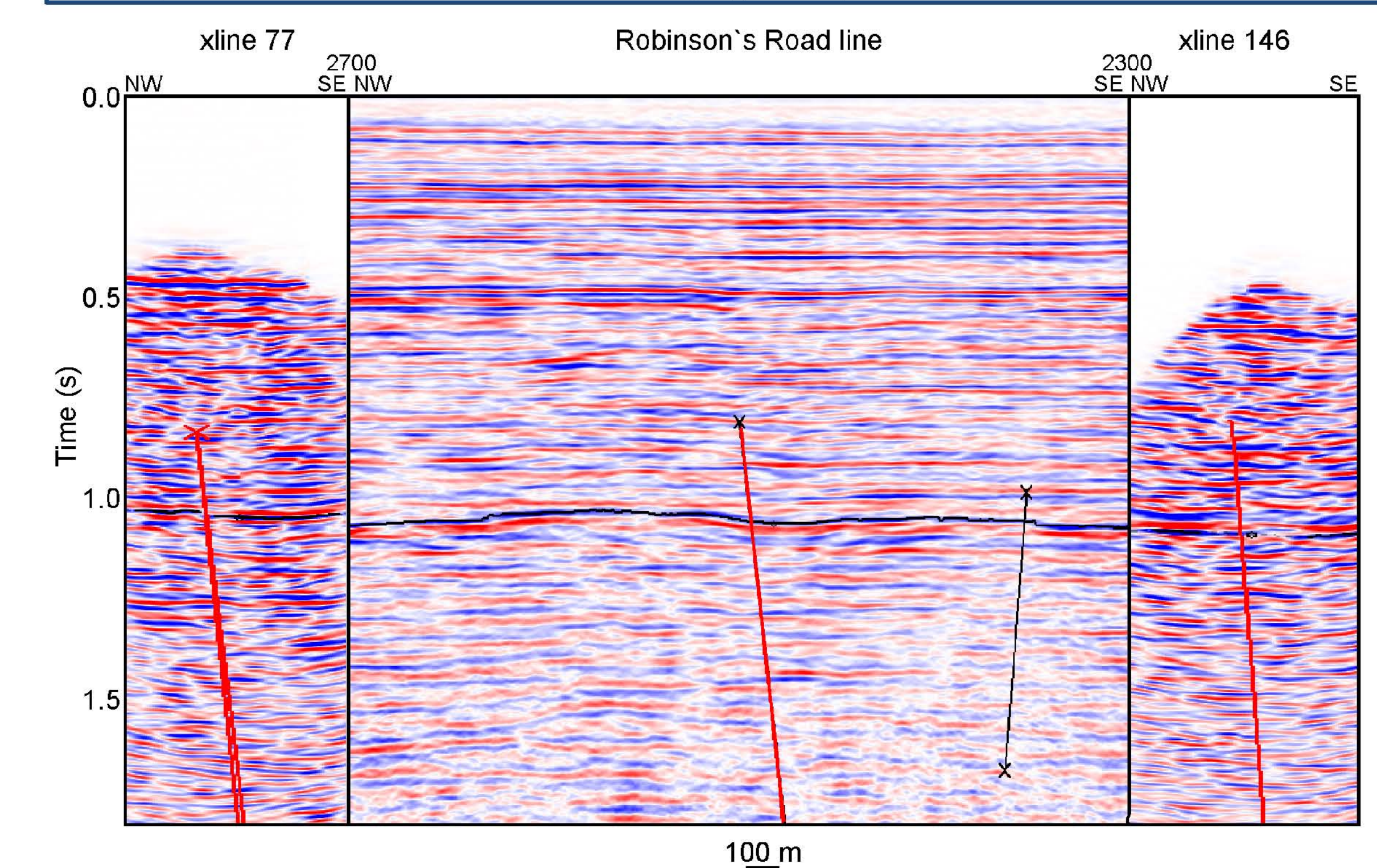

FIG. 8: Three semi-parallel lines: crossline 77, Robinson's Road 2D line and crossline 146. The red fault on the crosslines is interpreted to be the same one as the red fault interpreted previously (on Robinson's Road line and its trace is displayed on the map..
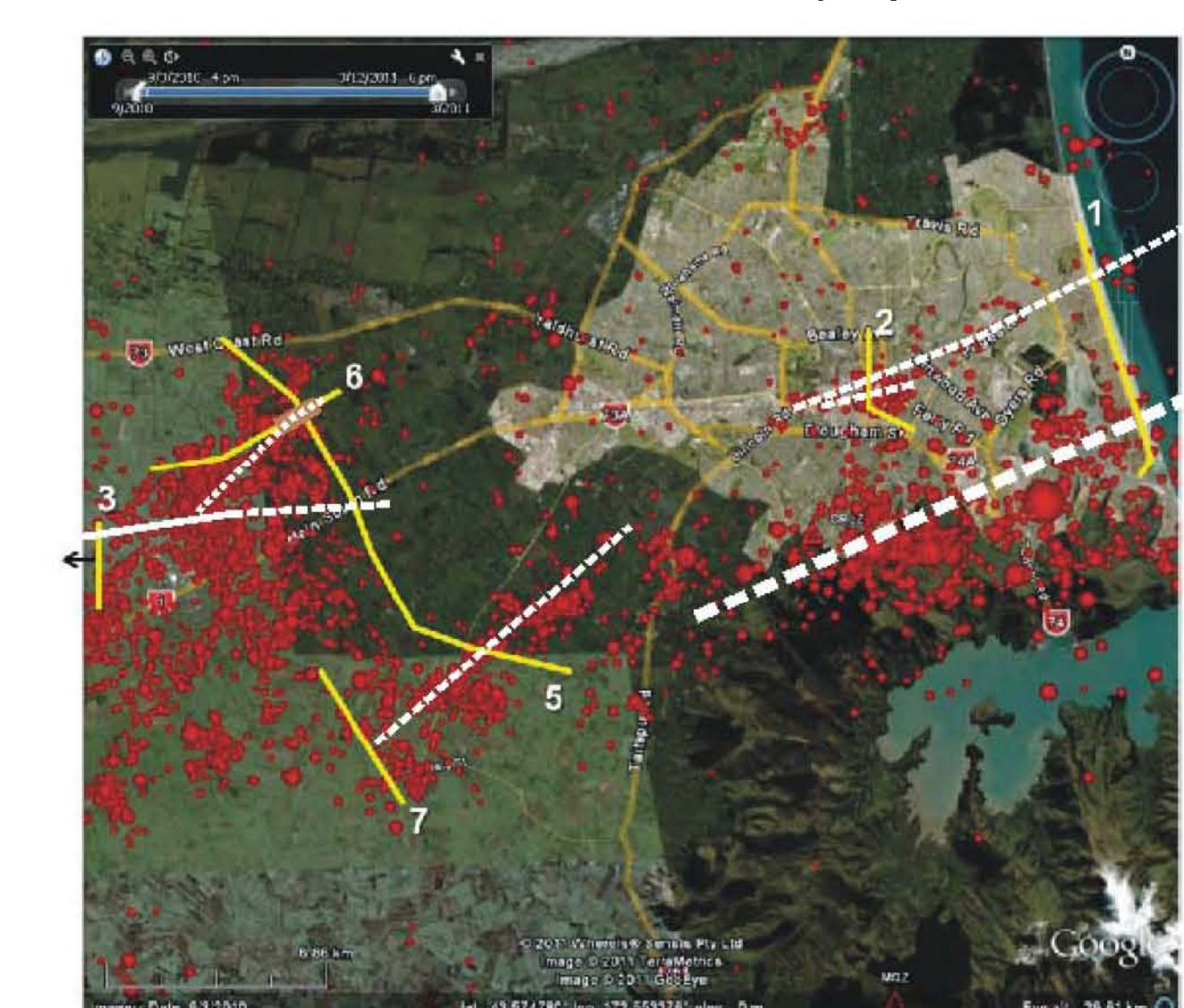

FIG 9: Map shown in Figure 1 with the adjusted trace of the fault cutting lines 5 and 6 based on the interpretation of the fault trace on the pseudo-3D survey (terracotta oblong).

CONCLUSIONS

By processing seismic data acquired by recording along a line orthogonal to a source line we were able to create a pseudo-3D seismic survey. Despite the low fold of the binned and stacked data, we were able to interpret a major fault on the pseudo-3D survey, to correlate this fault with one interpreted on the 2D surveys and to update the fault map

CREWES

NSERC CRSNG

UNIVERSITY OF CALGARY